NANOSYSTEMS: PHYSICS, CHEMISTRY, MATHEMATICS, 2020, 11 (4), P. 417–423

Synthesis of $NaYF_4$:Yb, Er up-conversion luminophore from nitrate flux

P. P. Fedorov[1*], M. N. Mayakova[1], A. A. Alexandrov[1], V. V. Voronov[1],
D. V. Pominova[1], E. V. Chernova[1], V. K. Ivanov[2]

[1]Prokhorov General Physics Institute of the Russian Academy of Sciences, 119991, Moscow, Russia
[2]Kurnakov Institute of General and Inorganic Chemistry of the Russian Academy of Sciences,
119991, Moscow, Russia

*ppfedorov@yandex.ru

PACS 81.07.Bc, 76.30.Kg **DOI 10.17586/2220-8054-2020-11-4-417-423**

The behavior of nanoparticle ensembles was studied using of $NaRF_4$ hexagonal phases. The evolution of particles in the process of rapid and productive synthesis from flux as a result of a chemical reaction was investigated. A low-temperature synthesis process in the medium of sodium nitrate was used. Synthesis of the samples of up-conversion phosphor $NaY_{0.78}Yb_{0.2}Er_{0.02}F_4$ was performed from rare-earth nitrates at 350 – 430 °C for 15 – 500 min. NaF was used as the fluorinating agent. Powder X-ray phase analysis and scanning electron microscopy revealed a rapid transformation of the cubic alpha modification into a hexagonal phase, followed by the transformation of nanoparticles into hexagonal prisms of micron sizes. The up-conversion luminescence energy yield increased as the reaction time increased.

Keywords: sodium yttrium fluoride, fluorite crystal structure, gagarinite crystal structure, flux, sodium nitrate.

Received: 15 April 2020

Revised: 30 April 2020

1. Introduction

The hexagonal phases formed in NaF–RF_3 (R – rare earth elements, REE) systems are effective matrices for anti-Stokes luminescence. They are phases of variable composition of the general formula $Na_{3x}R_{2-x}F_6$, and their composition is close to the ratio 50:50, according to which they are usually attributed the formula β-$NaRF_4$. These phases are low-temperature ones, as compare with cubic fluorite-type α-$NaRF_4$ phases. β-$NaRF_4$ phases, when co-doped with Yb–Er, Yb–Tm, or Yb–Ho ions, are well known as effective up-conversion phosphors that convert IR radiation to the visible spectral range [1, 2]. The number of publications devoted to these materials is huge, see for example [3–13]. The main areas of their potential application are biomedical applications and lighting sources [11–13]. The $NaY_{0.78}Yb_{0.2}Er_{0.02}F_4$ is the optimized composition. Functional characteristics of these materials depend strongly on the granulometry of the resulting nano- and micro-powders, and the mechanisms of phase formation, growth and agglomeration of particles are of crucial importance.

β-$NaRF_4$ powders can be prepared by a broad variety of methods [11, 13–16]. Until now, several techniques have been employed for the synthesis of hexagonal $NaRF_4$' phases, both individual and co-doped ones, including solid-state synthesis [14, 15, 17], co-precipitation from water [18–22] and organic solvents [23], hydrothermal [12, 24, 25], solvothermal [26–30], mechanochemical [31], ionic liquid-assisted [32, 33] and molten salt/flux methods [18, 33–43], etc.

Among the various methods of synthesis, much attention is drawn to the first melt-solution method proposed by Batsanova [18, 38, 44], which consists in the reaction of REE nitrates with sodium fluoride, which acts as a fluorinating agent. As a flux, low-melting sodium nitrate is used. The method is characterized by simple hardware design, high performance, environmental friendliness and low cost. We have shown [45] that in this way it is easy to obtain powders of equilibrium hexagonal phases formed in systems of sodium fluoride with REE fluorides RF_3 (R = Pr–Lu,Y).

The purpose of this work is to use this synthesis technique to prepare an up-conversion phosphor $NaYF_4$:Yb,Er and test its effectiveness.

2. Experimental details

2.1. Sample preparation

The samples were synthesized by spontaneous crystallization from a solution in a melt. The synthesis was based on the following equation:

$$R(NO_3)_3 + 4NaF \;\rightarrow\; NaRF_4\downarrow + 3NaNO_3. \qquad (1)$$

The starting chemicals were sodium fluoride (NaF, Lanhit®, purity mark "P.A."), yttrium nitrate hexahydrate ($Y(NO_3)_3 \cdot 6H_2O$, Lanhit®, purity 99.99 %), ytterbium nitrate hexahydrate ($Yb(NO_3)_3 \cdot 6H_2O$, Lanhit®, purity 99.99 %), erbium nitrate pentahydrate ($Er(NO_3)_3 \cdot 5H_2O$, Lanhit®purity 99.99 %) and sodium nitrate ($NaNO_3$, Chimmed Group, purity mark "CP") as a solvent. The raw materials were carefully mixed, transferred to a porcelain-glazed crucible, and placed in a furnace for synthesis. The ratio of components was: a seven-fold excess of the fluorinating agent from the stoichiometric composition (eq. 1), the mass fraction of the solvent ($NaNO_3$) was 35 %. The temperature range was from 320 to 350 °C (see Table 1). The heating speed was 10 °C/min for all samples. The sample holding time at the maximum temperature (τ, min) was from 15 to 500 minutes. The resulting residue was extracted from the crucible and washed several times with doubly distilled water.

TABLE 1. Synthesis conditions and hexagonal unit cell parameters of $NaY_{0.78}Yb_{0.2}Er_{0.02}F_{4.0}$ powders

No.	T, °C	τ, min	Unit cell parameters, Å	
			a	c
1	320	15	5.975(1)	3.5111(7)
2	330	30	5.9757(4)	3.5137(3)
3	340	45	5.9726(2)	3.5165(2)
4	350	60	5.9713(2)	3.5154(1)
5	350	180	5.9705(2)	3.5181(1)
6	350	500	5.9731(1)	3.5167(2)

2.2. Sample characterization

X-ray diffraction analysis (XRD) was performed on a Bruker D8 Advance diffractometer with Cu (Kα) radiation. The obtained data were processed by the TOPAS software package. When calculating the lattice parameters, the space group P63/m was set.

The Carl Zeiss NVision 40 electron microscope (Zeiss, Germany) was used for scanning electron microscopy (SEM) and energy dispersive X-ray spectroscopy (EDX) in high vacuum mode, at an accelerating voltage of 20 kV. Images were generated using a backscattered electron detector (BSE) and a secondary electron detector (SE).

The spectroscopic analysis included registering the spectra of up-conversion luminescence and diffusely scattered laser radiation within the range of 300 – 1000 nm, and calculating the energy yield of up-conversion luminescence. Luminescence studies were performed using a laser-induced luminescent spectroscopy unit that includes a fiber-optic spectroanalyzer LESA-01-BIOSPEC [46]. The values of the energy yield of up-conversion luminescence in the visible range of the spectrum were measured using a setup in which the test sample was placed in a modified integrating sphere produced by Avantes. Excitation of up-conversion luminescence was performed by a laser with a wavelength of 974 nm ("Biospek", Moscow, Russia) and a power of 1 W. Spectral data were analyzed using the UnoMomento spectrum processing program, taking into account the hardware function of the spectrometer and the integrating sphere.

3. Results and discussion

The results of XRD analysis are presented in Fig. 1. For a short synthesis time, a mixture of cubic and hexagonal phases is obtained. A half-hour exposure of the reaction mixture in the melt leads to the formation of a pure hexagonal phase. Further increase in the heat treatment duration does not lead to a change in the phase composition of the samples. The values of lattice parameters of hexagonal phase are presented in Table 1.

Electron microscopy data are shown on Figs. 2 and 3. The initially formed ensemble of nanoparticles (Fig. 2(a,b)) generates the formation of elongated particles of micron sizes. The grain size distribution of the samples is not uniform. Elongated particles have an approximately hexagonal faceting corresponding to their crystallographic symmetry. Trigonal prisms are distinguishable. However, microcrystals that are approximately characterized by these simple habit forms have a huge number of rough defects and are splices of smaller crystals. These results are similar to what we previously observed in the synthesis of $NaRF_4$ phases [45].

EDX data show that the actual composition of synthesized samples corresponds to the nominal one. Admixtures of other elements were not recorded.

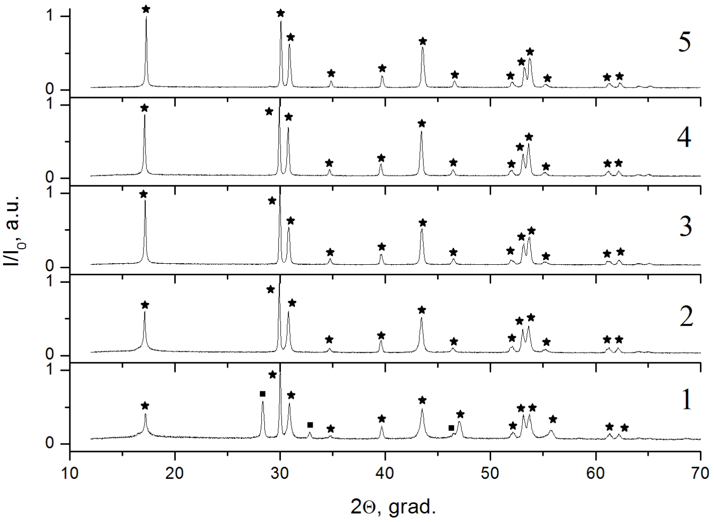

FIG. 1. X-ray powder diffraction patterns of the samples. Stars denote the peaks of the hexagonal $NaRF_4$ phase, and squares denote the cubic one. Sample numbers are the same as in the Table 1

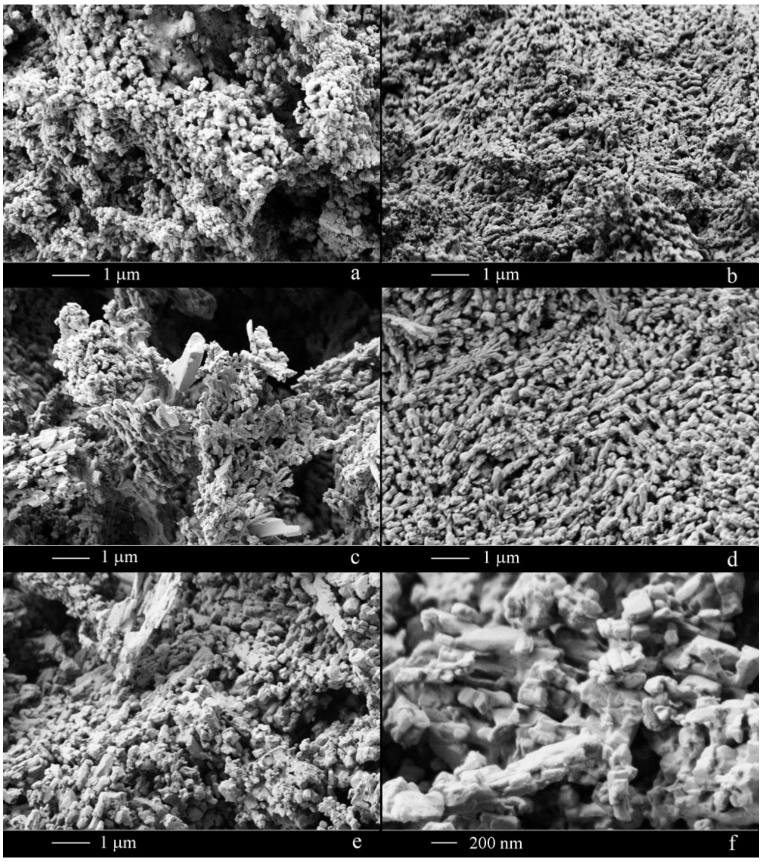

FIG. 2. SEM images of samples 1–3. (a) and (b) – the sample 1; (c) and (d) – the sample 2; (e) and (f) – the sample 3

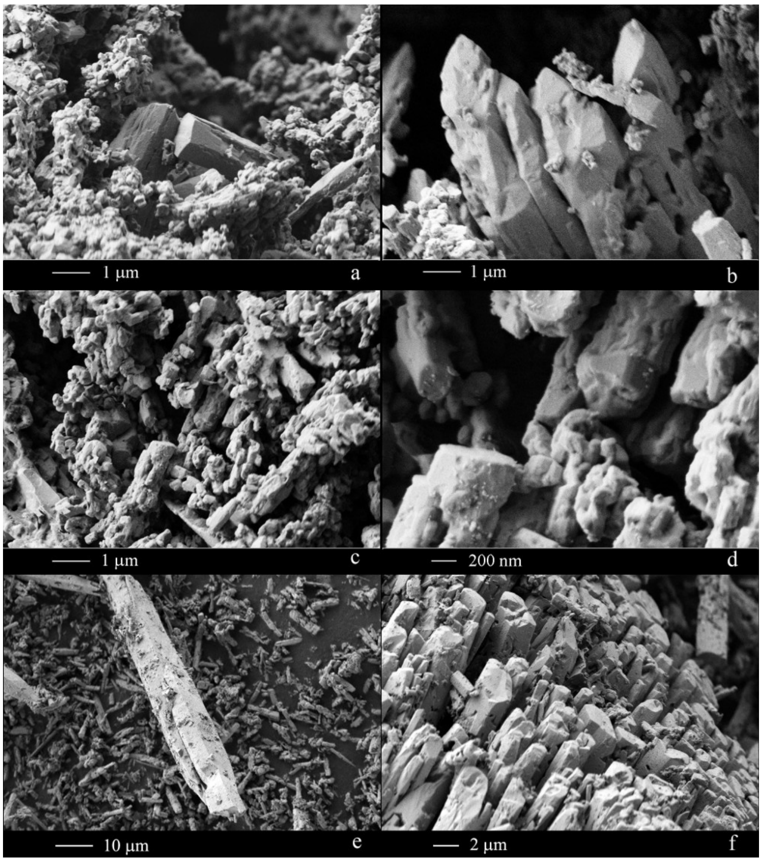

FIG. 3. SEM images of samples 4–6. (a) and (b) – the sample 4; (c) and (d) – the sample 5; (e) and (f) – the sample 6

It should be noted that the cubic α-phase is a high-temperature phase in NaF–RF_3 systems, and it is non-equilibrium one under our synthesis conditions. Cubic-hexagonal transitions ($\alpha \to \beta$ transitions) in $NaRF_4$ phases have been reported in the numerous publications describing $NaRF_4$ phase syntheses by a variety of techniques [4–11]. Temperature increase and/or extension of the synthesis duration promote the aforementioned $\alpha \to \beta$ phase transition. This transformation, which is also observed in our experiment when the thermal treatment time is increased to 30 min (see Fig. 1), is an actual realization of the Ostwald's step rule [47,48].

Bard et al. [12] attempted to interpret this transformation as a manifestation of non-classical crystal growth by the oriented attachment of nanoparticles. This assumption should be considered untenable [49]. In view of the different structures of α and β polymorphs, one should realize that beta-phase cannot be built from the pieces of the alpha-phase. A change in the coordination number (CN) of the rare earth ions (CN 8 for cubic α phase and CN 9 for hexagonal β phase) unequivocally requires complete recrystallization of the formed cubic nanoparticles.

On the other hand, the enlargement of beta phase particles during thermal annealing fits well into the scheme of non-classical crystal growth by agglomeration of particles [50,51]. The poor faceting of the formed crystallites is a confirmation of this [52].

The results of the luminescent studies are presented on the Fig. 4 and in the Table 2.

The luminescence spectra of the samples are typical for this luminophore and show green (510 – 575 nm) and red (625 – 670 nm) bands, corresponding to the radiative transitions of the erbium ions: ${}^2H_{11/2}$, ${}^4S_{3/2} \to {}^4I_{15/2}$ and ${}^4F_{9/2} \to {}^4I_{15/2}$, respectively.

Changes in the synthesis duration had a tangible effect on luminescence efficiency of the samples. As the exposure time increased, the energy yield of up-conversion luminescence increased monotonously. At the same time, the ratio of red and green luminescence bands changed slightly.

The results shown in the Table 2 allow the following conclusions. The difference in the values of energy yield may be accounted for by the larger size of the particles (resulting from the longer synthesis), which leads to an increase in the surface area-to-volume ratio. Similar phenomena (surface quenching effect) have been observed for upconversion $NaGdF_4$:Yb,Tm nanoparticles [53] and for the intrinsic exciton luminescence in MF_2 nanocrystals also [54,55].

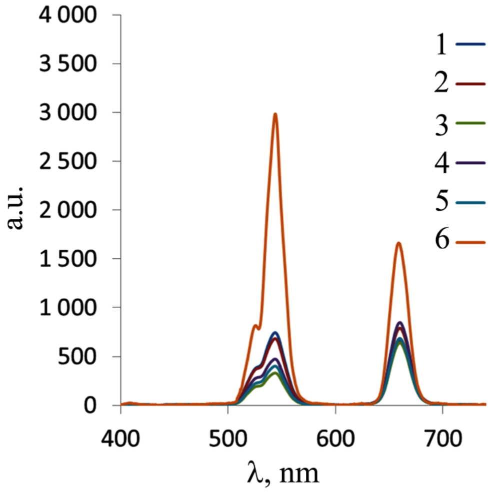

FIG. 4. Luminescence spectra of samples 1–6. The wavelength of the pumping laser is 974 nm

TABLE 2. Estimated external energy yield (EQ) of up-conversion luminescence of Er^{3+} ions of $NaY_{0.78}Yb_{0.20}Er_{0.02}F_{4.0}$ powder samples measured in integrating sphere, %

No.	EQ,%	EQ_1 %, red band	EQ_2 %, green band	EQ_1/ EQ_2
1	0.73	0.0033	0.0040	0.80
2	0.85	0.0044	0.0041	1.06
3	0.50	0.0032	0.0019	1.70
4	0.68	0.0041	0.0027	1.54
5	0.57	0.0034	0.0023	1.50
6	2.25	1.08	1.17	0.92

4. Conclusion

Our studies have shown the possibility of synthesizing an effective up-conversion phosphor $NaYF_4$:Yb, Er by a chemical reaction in a sodium nitrate flux. The target hexagonal phase is formed from the primary non-equilibrium cubic nanophase in accordance with the Ostwald's step rule. The resulting particles quickly grow in size with the formation of micron-sized particles that have a rough hexagonal habit with strong symmetry violations and multiple defects. The implementation of a non-classical mechanism of crystal growth by directed agglomeration of particles is assumed. An increase in the particle size results in an increase in the efficiency of up-conversion luminescence.

Acknowledgements

The work was preformed under the RFBR grant 18-29-12050mk. The authors are grateful to Dr. A. E. Baranchikov for his assistance in conducting research and to Dr. S. V. Kuznetsov for helpful discussions. All experiments were performed on the equipment kindly provided by the Centre for Collective Use of Prokhorov General Physics Institute of the Russian Academy of Sciences and the Centre for Collective Use of Kurnakov Institute of General and Inorganic Chemistry of the Russian Academy of Sciences.

References

[1] Ovsyankin V.V., Feofilov P.P. On the mechanism ofcombination of electron excitations in activatedcrystals. *JETP Lett.*, 1966, **3**, P. 322–323.

[2] Auzel F.E. Compteur quantique par transfert denergie entre deux ions de terres rares dans un tungstate mixte et dans un verre. *C. R. Acad. Sci. B*, 1966, **262**, P. 1016–1019.

[3] Krämer K., et al. Hexagonal Sodium Yttrium Fluoride Based Green and Blue Emitting Upconversion Phosphors. *Chemistry of Materials*, 2004, **16**, P. 1244–1251.

[4] Mai H.-X., et al. Size- and Phase-Controlled Synthesis of Monodisperse $NaYF_4$:Yb,Er Nanocrystals from a Unique Delayed Nucleation Pathway Monitored with Upconversion Spectroscopy. *The Journal of Physical Chemistry C*, 2007, **111**, P. 13730–13739.

[5] Li C., et al. Two-Dimensional -$NaLuF_4$ Hexagonal Microplates. *Crystal Growth & Design*, 2008, **8**, P. 923–928.

[6] Zhang F., et al. Shape, Size, and Phase-Controlled Rare-Earth Fluoride Nanocrystals with Optical Up-conversion Properties. *Chemistry European Journal*, 2009, **15**, P. 11010–11019.

[7] Yang L.V., et al. White emission by Frequency Up-Conversion in Yb^{3+}–Ho^{3+}–Tm^{3+} Triply Doped Hexagonal $NaYF_4$ Nanorods. *The Journal of Physical Chemistry C*, 2009, **113**, P. 18995–18999.

[8] Zhang F., et al. Photoluminescence Modification in Upconversion Rare-Earth fluoride Nanocrystal Array Conducted Photonic Crystals. *Journal of Materials Chemistry*, 2010, **20**, P. 3895–3900.

[9] Liu Q., et al. Sub-10nm Hexagonal Lanthanide-Doped $NaLuF_4$ Upconversion Nanocrystals for Sensitive Bioimaging in Vivo. *Journal American Chemical Society*, 2011, **133**, P. 17122–17125.

[10] Nordmann J., et al. Synthesis of ß-Phase $NaYF_4$:Yb,Er Upconversion Nanocrystals and Nanorods by Hot-Injection of Small Particles of the α-Phase. *Zeitschrift für Physikalische Chemie*, 2015, **229**, P. 247–262.

[11] Naccache R., Yu Q., Capobianco A. The Fluoride Host: Nucleartion, Growth, and Upconversion of Lanthanide-Doped Nanoparticles. *Advanced Optical Materials*, 2015, **3**, P. 482–509.

[12] Bard A.B., et al. Mechanistic Understanding of Non-Classical Crystal Growth in Hydrothermally Synthesized Sodium Yttrium Fluoride Nanowires. *Chemistry of Materials*, 2020, **32** (7), P. 2753–2763.

[13] Fedorov P.P., Luginina A.A., Kuznetsov S.V., Osiko V.V. Nanofluorides. *Journal of Fluorine Chemistry*, 2011, **132** (12), P. 1012–1039.

[14] *Gmelin Handbuch der anorganischen Chemie. Syst. Nummer 39: Seltenerdelemente*. Teil C3: Sc, Y, La und Lanthanide. Fluoride, Oxifluoride und zugehogige Alkalidoppelverbindungen. Berlin, Springer Vlg., 1976.

[15] Sobolev B.P. *The Rare Earth Trifluorides. Part 1. The High Temperature Chemistry of the Rare Earth Trifluorides*. Institut d'Estudis Catalans, Barcelona, Spain, 2000.

[16] Fedorov P.P., Luginina A.A., Popov, A.I. Transparent oxyfluoride glass ceramics. *J. Fluor. Chem.*, 2015, **172**, P. 22–50.

[17] Fedorov P.P. Systems of Alcali and Rare-Earth Metal Fluorides. *Russian Journal of Inorganic Chemistry*, 1999, **44**, P. 1703–1727.

[18] Batsanova L.R. Rare-earth fluorides. *Russ. Chem. Rev.*, 1971, **40** (6), P. 465–484.

[19] Fedorov P.P., Kuznetsov S.V., et al. Coprecipitation from aqueous solutions to prepare binary fluorides. *Russ. J. Inorg. Chem.*, 2011, **56**, P. 1525–1531.

[20] Fedorov P.P., et al. Soft Chemical Synthesis of $NaYF_4$ Nanopowders. *Russian Journal Inorganic Chemistry*, 2008, **53**, P. 1681–1685.

[21] Yi G.S., Lu H.C., et al. Synthesis, Characterization, and Biological Application of Size-Controlled Nanocrystalline $NaYF_4$:Yb, Er Infrared-to-Visible Up-Conversion Phosphors. *Nano Lett.*, 2004, **4**, P. 2191–2196.

[22] Cao C., Zhang X., et al. Ultraviolet and blue up-conversion fluorescence of $NaY_{0.793x}Tm_{0.007}Yb_{0.2}Gd_xF_4$ phosphors. *J. Alloys Compd.*, 2010, **505** (1), P. 6–10.

[23] Wang F., Deng R., Liu X. Preparartion of core-shell $NaGdF_4$ nanoparticles doped with luminescent lanthanide ions to be used as upconversion-based probes. *Nature Protocol*, 2014, **9**, P. 1634–1644.

[24] Sobolev B.P., Mineev D.A., Pashutin V.P. Low-temperature hexagonal polymorph $NaYF_4$ with gagarinite-type structure. *Dokl. AN SSSR*, 1963, **150**, P. 791–794 (in Russian).

[25] Liang L.F., Wu H., et al. Enhanced blue and green upconversion in hydrothermally synthesized hexagonal $NaY_{1x}Yb_xF_4$:Ln^{3+} (Ln^{3+} = Er^{3+} or Tm^{3+}). *J. Alloys Compd.*, 2004, **368**, P. 94–100.

[26] Wang Q., Tan M.C., et al. A Solvothermal Route to Size- and Phase-Controlled Highly Luminescent $NaYF_4$:Yb, Er Up-Conversion Nanocrystals. *J. Nanosci. Nanotechnol.*, 2010, **10** (3), P. 1685–1692.

[27] Liu J-N., Bu W., et al. Simultaneous nuclear imaging and intranuclear drug delivery by nuclear-targeted multifunctional upconversion nanoprobes. *Biomaterials*, 2012, **33** (29), P. 7282–7290.

[28] Chen F., Bu W., et al. Gd^{3+}IonDoped Upconversion Nanoprobes: Relaxivity Mechanism Probing and Sensitivity Optimization. *Adv. Funct. Mater.*, 2013, **23** (3), P. 298–307.

[29] Guo J., Ma F., et al. Solvothermal synthesis and upconversion spectroscopy of monophase hexagonal $NaYF_4$:Yb^{3+}/Er^{3+} nanosized crystallines. *J. Alloys Compd.*, 2012, **523**, P. 161–166.

[30] Yu S., Wang Z., Gao R., Meng L. Microwave-assisted synthesis of water-disperse and biocompatible $NaGdF_4$:Yb,Ln@$NaGdF_4$ nanocrystals for UCL/CT/MR multimodal imaging. *J. Fluorine Chem.*, 2017, **200**, P. 77–83.

[31] Lu J., Zhang Q., Saito F. Mechanochemical synthesis of Nano-sized complex fluorides from pair of different constituent fluoride compounds. *Chem. Letters*, 2002, **31** (12), P. 1176–1770.

[32] Bartůněk V., Pinc J., et al. Tunable rapid microwave synthesis of up-converting hexagonal $NaY_xGd_yYb_zEr_{(1-x-y-z)}F_4$ nanocrystals in large quantity. *J. Fluor. Chem.*, 2015, **178**, P. 56–60.

[33] Fedorov P.P., Alexandrov A.A. Synthesis of Inorganic Fluorides from Molten Salt Fluxes and Ionic Liquid Mediums. *J. Fluorine Chem.*, 2019, **227**, 109374.

[34] Suzuki S., Teshima K., et al. Low-Temperature Flux Growth and Upconversion Fluorescence of the Idiomorphic Hexagonal-System $NaYF_4$ and $NaYF_4$:Ln (Ln = Yb, Er, Tm) Crystals. *Cryst. Growth Des.*, 2011, **11** (11), P. 4825–4830.

[35] Suzuki S., Teshima K., et al. Novel fabrication of NIR-vis upconversion $NaYF_4$:Ln (Ln = Yb, Er, Tm) crystal layers by a flux coating method. *J. Mater. Chem.*, 2011, **21**, P. 13847–13852.

[36] Ding M., Chen D., et al. Molten salt synthesis of ß-$NaYF_4$:Yb^{3+},Ln^{3+}, (Ln = Er, Tm, and Ho) micro/nanocrystals with controllable morphology and multicolor upconversion luminescence. *Sci Adv. Mater.*, 2017, **9**, P. 688–695.

[37] Zhang X., Yang P., et al. Facile and mass production synthesis of ß-$NaYF_4$:Yb^{3+},Er^{3+}/Tm^{3+} 1D microstructures with multicolor up-conversion luminescence. *Chem. Commun.*, 2011, **47** (44), P. 12143–12145.

[38] Batsanova L.R., Kupriyanova A.K., Doroshenko V.I. Study of the interaction of the rare-earth nitrates with sodium fluorides in molten $NaNO_3$. *Inorg. Mater.*, 1971, **7**, P. 1876–1877 (In Russian).

[39] Suzuki S., Teshima K., et al. Novel fabrication of NIR-vis upconversion $NaYF_4$:Ln (Ln = Yb, Er, Tm) crystal layers by a flux coating method. *J. Mater. Chem.*, 2011, **21**, P. 13847–13852.

[40] Suzuki S., Teshima K., et al. Low-temperature flux growth and upconversion fluorescence of the idiomorphic hexagonal-system $NaYF_4$ and $NaYF_4$:Ln (Ln = Yb, Er, Tm) crystal. *Cryst. Growth. Des.*, 2011, **11**, P. 4825–4830.

[41] Zhang X., Yang P., et al. Facile and mass production synthesis of ß-$NaYF_4$:Yb^{3+}, Er^{3+}/ Tm^{3+} 1D microstructures with multicolor up-conversion luminescence. *Chem. Commun.*, 2011, **47**, P. 12143–12145.

[42] Ding M., Lu C., et al. Facile synthesis of ß-$NaYF_4$:Ln^{3+}(Ln = Eu, Tb, Yb/Er, Yb/Tm) microcrystals with down- and up-conversion luminescence. *J. Mater. Sci.*, 2013, **48**, P. 4989–4998.

[43] Huang X.Y., Hu G.H., et al. Molten-salt synthesis and upconversion of hexagonal $NaYF_4$:Er^{3+}:Yb^{3+} micro-/nano-crystals. *J. Alloys Compd.*, 2014, **616**, P. 652–661.

[44] Fedorov P.P., et al. The melt of sodium nitrate as a new medium for synthesis of fluorides. *Inorganics*, 2018, **6**, P. 38–55.

[45] Fedorov P.P., et al. Preparation of "$NaRF_4$" phases from the sodium nitrate melt. *J. Fluorine Chem.*, 2019, **218**, P. 69–75.

[46] Ryabova A. V., et al. Spectroscopic research of upconversion nanomaterials based on complex oxide compounds doped with rare-earth ion pairs: Benefit for cancer diagnostics by upconversion fluorescence and radio sensitive methods. *Photon Lasers Med.*, 2013, **2**, P. 117–128.

[47] Ostwald W. Studien über die Bildung und Umwandlung fester Körper. *Zeitschrift fr Physikalische Chemie*, 1897, **22**, P. 289–330.

[48] Threlfall T. Structural and thermodynamics explanation of Ostwalds rule. Organic Process Research and Development. 2003, 7, P. 1017–1027.

[49] Fedorov P.P. Comment on the paper A.B. Bard, X. Zue, G. Zhu, et al. A Mechanistic Understanding of Non-Classical Crystal Growth in Hydrothermally Synthezied Sodium Yttrium Fluoride Nanowires. *Chem. Mat.*, 2020, accepted for publication.

[50] Ivanov V.K., Fedorov P.P., Baranchikov A.Y., Osiko V.V. Oriented Aggregation of Particles: 100 Years of Investigations of Non-Classical Crystal Growth. *Russian Chemical Review*, 2014, **83**, P. 1204–1222.

[51] De Yoreo J.J., et al. Crystallization by particle attachment in synthetic, biogenic, and geologic environments. *Science*, 2015, **349** (6247), aaa6760.

[52] Fedorov P.P., Osiko V.V. Relationship between the Faceting of Crystals and Their Formation Mechanism. *Doklady Physics*, 2019, **64** (9), P. 353–355.

[53] Wang F., Wang J., Liu X. Direct evidence of a surface quenching effect on size-dependent luminescence of upconversion nanoparticles. *Angew. Chem. Int. Ed.*, 2010, **49**, P. 7456–7460.

[54] Demkiv T., et al. Intrinsic luminescence of SrF_2 nanoparticles. *Journal of Luminescence*, 2017, **190**, P. 10–15.

[55] Vistovskyy V.V., et al. The luminescence of BaF_2 nanoparticles upon high-energy excitation. *Journal of Applied Physics*, 2014, **116**, 054308.